Minimum reaction network necessary to describe Ar/CF4 plasma etch

Helpert, Sofia, Chopra, Meghali, Bonnecaze, Roger

Sofia Helpert, Meghali Chopra, Roger T. Bonnecaze, "Minimum reaction network necessary to describe Ar/CF4 plasma etch," Proc. SPIE 10589, Advanced Etch Technology for Nanopatterning VII, 105890J (20 March 2018); doi: 10.1117/12.2297502

SPIE.

Event: SPIE Advanced Lithography, 2018, San Jose, California, United States

Minimum reaction network necessary to describe Ar/CF_4 plasma etch

Sofia Helpert[a], Meghali Chopra[a,b,*], Roger T. Bonnecaze[a,b]
[a]McKetta Department of Chemical Engineering, The University of Texas at Austin, 200. E. Dean Keeton, Austin, TX 78712;
[b]SandBox Semiconductor, 300 N. Lamar 136, Austin, TX 78703

ABSTRACT

Predicting the etch and deposition profiles created using plasma processes is challenging due to the complexity of plasma discharges and plasma-surface interactions. Volume-averaged global models allow for efficient prediction of important processing parameters and provide a means to quickly determine the effect of a variety of process inputs on the plasma discharge. However, global models are limited based on simplifying assumptions to describe the chemical reaction network. Here a database of 128 reactions is compiled and their corresponding rate constants collected from 24 sources for an Ar/CF_4 plasma using the platform RODEo (**R**ecipe **O**ptimization for **D**eposition and **E**tching). Six different reaction sets were tested which employed anywhere from 12 to all 128 reactions to evaluate the impact of the reaction database on particle species densities and electron temperature. Because many the reactions used in our database had conflicting rate constants as reported in literature, we also present a method to deal with those uncertainties when constructing the model which includes weighting each reaction rate and filtering outliers. By analyzing the link between a reaction's rate constant and its impact on the predicted plasma densities and electron temperatures, we determine the conditions at which a reaction is deemed necessary to the plasma model. The results of this study provide a foundation for determining which minimal set of reactions must be included in the reaction set of the plasma model.

Keywords: reaction networks, plasma etching, global plasma model

1. INTRODUCTION

Computational modeling of plasma etch systems offers a number of benefits towards the advancement of plasma processing for next–generation technologies. The performance of different reactor configurations can be predicted and assessed prior to implementation and vast multi-dimensional process spaces can easily be explored to help achieve process objectives like selectivity, anisotropy, and uniformity. Extensive work has been performed on the development plasma models ranging from reactor scale to feature scale models and down to molecular dynamic simulations.[1-4]

Global plasma models are especially advantageous because they are fast and flexible.[4, 5] In a global plasma model, all plasma densities are assumed to be volume averaged. A power balance which includes energy losses from electron-neutral collisions and wall reactions is solved alongside a particle balance to determine electron temperatures. Accordingly, one of the most critical components in a global plasma model is the definition of the reaction network and the associated chemical kinetics for the plasma. This reaction network includes electron impact and ionization reactions, recombination reactions, charge transfer reactions, and surface loss reactions.

The complexity of a plasma system means that for even the simplest molecular plasmas, there can be dozens to hundreds of possible reactions that can be included in the reaction network of the global model. It is extremely challenging to determine which reactions are most important for accurately modeling the plasma system. Previously, a useful chemistry has been defined as one in which: (1) the chemistry is complete, (2) the reactions are balanced, and (3) the chemistry is correct.[6] To determine if a chemistry is correct, results must be verified experimentally—a long and arduous process. For self-consistent global plasma models, this problem is magnified even further as energy losses must be computed based on difficult to find (and experimentally measure) cross-sectional data.

What is perhaps even more challenging than selecting the appropriate reactions for inclusion in the reaction network is the calculation of the rate constants. Rate constants in literature vary widely. In Figure 1, rate constants are reported for

* meghali.chopra@sandboxsemiconductor.com

Advanced Etch Technology for Nanopatterning VII, edited by Sebastian U. Engelmann, Richard S. Wise,
Proc. of SPIE Vol. 10589, 105890J · © 2018 SPIE · CCC code: 0277-786X/18/$18 · doi: 10.1117/12.2297502

the reaction Ar + e → Ar^+ + 2e from nine different sources[7-15]. The illustrated reaction rates vary by as much as four orders of magnitude for the same reaction!

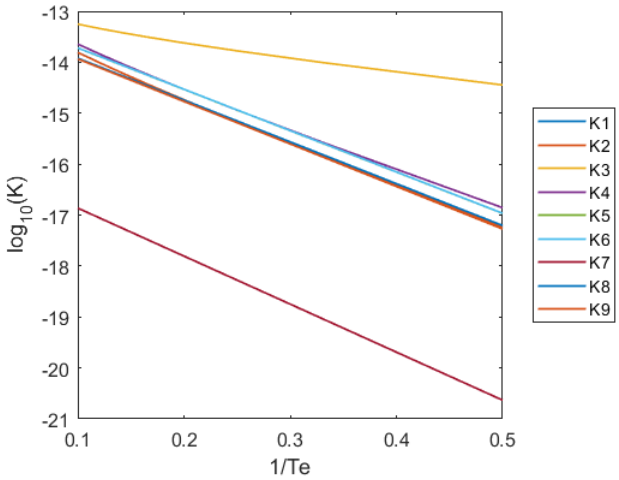

Figure 1. 1/Te versus the log of the rate constants for the reaction e + Ar → Ar^+ + 2e are reported from 9 different sources.

In this study we accomplish two objectives. First, we evaluate a statistical approach for dealing with uncertainty using weighted reaction rates. Second, we identify the minimum reaction network necessary to accurately capture the plasma process physics. The Ar/CF_4 reaction database in the platform "Recipe Optimization for Deposition and Etching" or RODEo, a plasma etch process simulation platform, was used to build the 6 different reaction networks described below.

2. METHODS

The global plasma models employed in all of the reaction sets consisted of a set of particle balances and a power balance.[4] All models were solved assuming a reactor of radius 0.15 m and length 0.14 m at a pressure of 15 mTorr, power of 700 W, and total input flow rate of 20 sccm.[19] The RODEo reaction database for Ar/CF_4 contains 149 bulk reactions derived from 24 sources.[4, 7-29] When constructing the Full-Model set, it was found that wall reactions were essential to producing realistic parameter values, and that including an excitation reaction in the bulk plasma for which there was no corresponding deexcitation rate constant in the database severely inhibited numerical convergence. Therefore, the full set of reactions was defined as that which included excitation reactions in the power balance, but not in the particle balance. The exceptions to this rule are the Ar metastable, resonant, and 4p excited states since they had deexcitation reactions as well as many other reactions in which they were consumed or produced (31 reactions in total). We also exclude double ionization reactions because their elementary steps are already included.

Wall loss rates ν_i of positive ions n_i were calculated such that

$$\nu_i n_{i0} = \Gamma_i \frac{A}{V}, \tag{1}$$

where A is the surface area of the cylindrical reactor and V is the volume. Similarly, neutral wall loss rates ν_N were determined by

$$\nu_N n_{N0} = \Gamma_N(l_p)\frac{A}{V}. \tag{2}$$

where l_p is the half-length of the system. Further details on how to calculate wall loss rates for plasma reactors are covered extensively in literature.[4, 5, 18, 30]

So, as all sets use the excitation reactions in the power balance, the Full model set was defined as having 128 reactions; 18 wall reactions and 110 bulk reactions. From this Full set, we consider six cases as listed in Table 1.

For many reactions, there are multiple reported rate constants from different literature sources. In the so-called Reaction Sets Full - 1 and Full - 2, the rate constants are determined using weights, without or with outliers, respectively. In Reduced - 1 and Reduced - 2, subsets of the bulk reactions are included in which reactions whose weighted rate

constants are below a certain threshold are removed. Minimal - 1 and Minimal - 2 are networks of 12 reactions using either weighted rate constants or a single rate constant[19].

Table 1. Reaction sets considered from RODEo database and the method employed to calculate the reaction rates for each set. "U" refers to all the Ar/CF_4 reactions in the RODEo database. " ⊂ " refers to the subset of reactions pulled from prior work to define the minimal reaction set.

Reaction Set Name	Number of Reactions (n)	Reactions Selected	Rate Constant Method
Full - 1	128	U	Weighted (without outliers)
Full - 2	128	U	Weighted (with outliers)
Reduced - 1	109	$\{k \mid k > \mu_k - \sigma_k\}$	Weighted
Reduced - 2	89	$\{k \mid k > \mu_k - 0.25\sigma_k\}$	Weighted
Minimal - 1	12	⊂	Weighted
Minimal - 2	12	⊂	Single Rate Constant formula[19]

2.1 Outlier Filtering

To determine outliers in reactions with multiple rate constant formulas, plots were created to view the behavior of each formula for one given reaction. Those that were orders of magnitude away from the population of reactions, or that had a noticeable difference in slope, were eliminated from the database. Weights were not considered for the elimination of outliers. Some reactions consisted of two different constant values that were orders of magnitude apart. As there was no way to decide on one over the other, both remained in the set.

2.2 Calculation of Weighted Rate Constants

To calculate the weighted reaction rate, the frequency of each formula in the reaction database was first counted to give priority to more commonly reported reactions. In reactions in which two constant values with differing orders of magnitude appeared, the greater order of magnitude is favored.

Simulations were run using different sets of reactions or different methods of calculating rate constants using the Full and Minimal sets. We show the effect of outlier rate constant formulas by comparing Full – 1 with Full – 2 which included the outlier reactions. We also show the effect of employing weighted rate constants by comparing Minimal – 1 with Minimal – 2 which used single reaction rate constants found in literature. [19]

2.3 Calculation of Reaction Rate Thresholds

To determine which reactions to use in each reaction set, reaction rates were filtered based on the speed of their respective rate constants. A histogram was constructed for the $\log_{10}(K)$ of the 110 bulk reactions, Reaction rates were first calculated using the electron temperature of Full – 1 at a CF_4 fraction of 0.5. The rates were then homogenized to have units of 1/sec by multiplying the calculated rate constant by the input flow rate to the power of the reaction order. Then, outliers were determined by the generalized extreme Studentized deviate (gesd) test for outliers in MATLAB. The two reactions with the lowest $\log_{10}(K)$ value were deemed outliers and removed from the distribution. The resulting histogram was then fit to a normal distribution. The histogram and normal probability distribution are shown in Figure 2 with the identified outliers at $\log_{10}(K) = -20.2$ and $\log_{10}(K) = -8.40$. The mean $\log_{10}(K)$ value was 3.53 and the standard deviation 2.97. These parameters were used to establish threshold rate constants such that all reaction rates faster than the thresholds were used. Once the bulk reactions were chosen, all wall reactions were added to produce a set with n reactions. The thresholds were chosen to be 0.25 ($n = 89$), and 1.0 ($n = 109$) standard deviations below the mean.

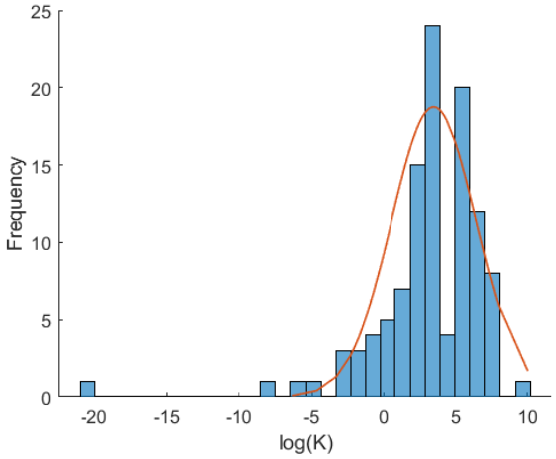

Figure 2. Histogram of reaction rates for all reactions included in the RODEo database (128 in total).

3. RESULTS

Figure 3 are plots of the predictions of electron temperature and electron density versus CF_4 fraction using Full - 1 and Full - 2. Removing outliers (Full - 1) produces much better agreement with the experimental measurements for electron temperature. Full - 1 also gives qualitatively better agreement than Full- 2 for the electron density at low values of CF_4. The full model with no outliers, which has no adjustable parameters, predicts the electron temperature within about 30% and the electron density within a factor of four. The discrepancy is attributed to the wall reactions and depends on the specific internals of the reactor. Overall, the 128 reactions in Reaction Set Full-1 capture the qualitative behavior of the

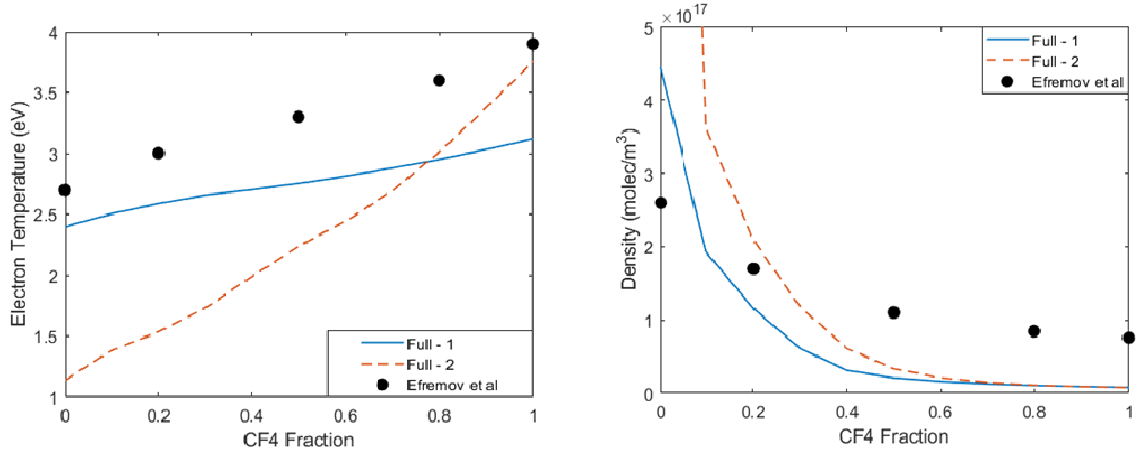

Figure 3. Comparison of electron temperature (left) and electron density (right) predicted by the reaction networks Full - 1 and Full - 2. Predictions are compared with experimentally measured electron temperatures and densities.19

electron temperature and density and quantitatively predict the results well within an order of magnitude with CF_4 fraction. We use this set as the standard to compare reduced models with fewer reactions.

In contrast to the 128 reaction full model, there are the 12 reaction minimal models. Figure 4 shows how this model compares to the experimental measurements of electron density and electron temperature. The minimal models do not differ much from one another. That is, the averaging of rate constants versus the selection of a single rate constant does not make much of a difference in the predictions. This is because the rate constants for this minimal model are well-studied and well-established. The minimal models qualitatively predict the electron density and match as well as the full model. While the minimal models qualitatively predict the correct trend for electron temperature for increasing CF_4, the full model is slightly better. The results indicate that the weighted method employed can be used to successfully model a plasma system where there are conflicting reaction rates.

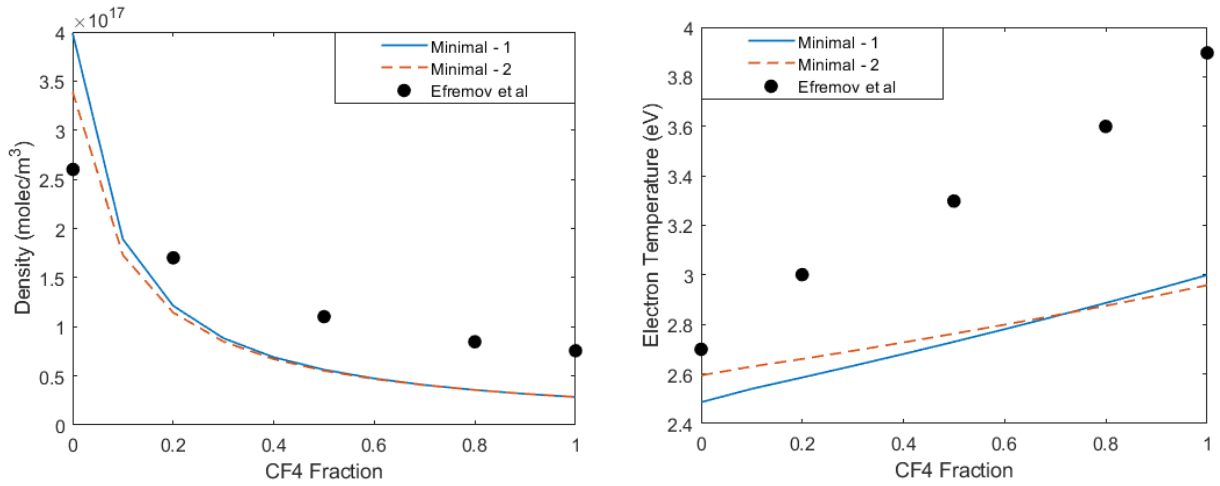

Figure 4. Comparison of weighted rate constants versus single rate constant with 12 reaction set. Electron density (left) and electron temperature (right).

We now compare the predictions of the number density of Ar^+, CF_3^+, F, the electron density and the electron temperature from the Full model (128 equations and outliers removed), and reduced versions with 109 and 89 reactions and the predictions of the minimal model to discern their variations. Figure 5 shows the variations number density of the positive ions as a function of the CF_4 fraction. All four kinetic models qualitatively predict the number density of Ar^+ to decrease with increasing CF_4 fraction. The predicted number densities are similar in magnitude. In general, the more complex the model the faster the number density of positive argon ions decreases with CF_4 fraction. The minimal model decreases noticeably slower than the other models. The difference between the minimal model and the other ones is much more noticeable for the number density of CF_3^+ . The minimal model predicts a monotonic increase with the CF_4 fraction, which is qualitatively different than the maxima predicted by the full and reduced models of the reaction network. The magnitude of the maxima and its location varies considerably among the full and reduced models.

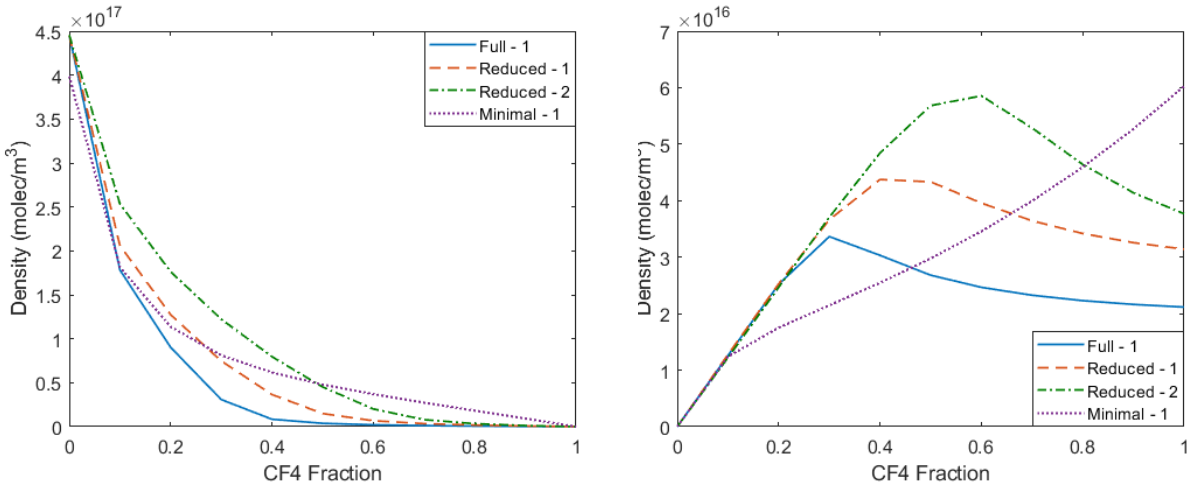

Figure 5. Number density of Ar^+ (left) and CF_3^+ (right) using the Full model (128 equations and outliers removed), and reduced versions with 109 and 89 reactions and the predictions of the minimal model.

A similar trend is seen for the number density of F in Figure 6. Again, the minimal model shows the number density increasing with increasing CF4 fraction. In sharp contrast, the number density of F exhibits maxima for the other models with varying locations and magnitudes.

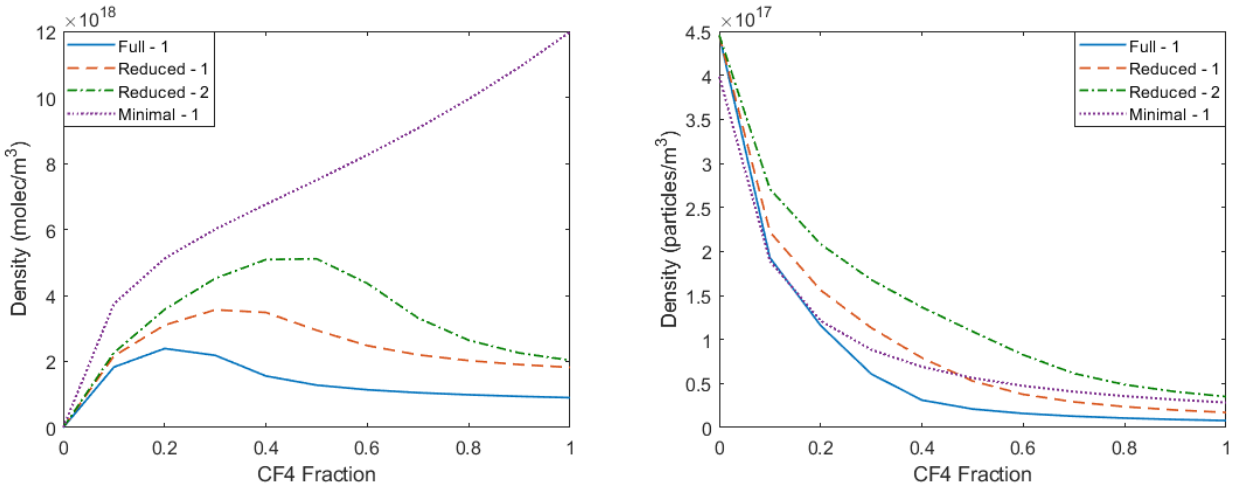

Figure 6. Number density of F (left) and electron density (right) using the Full model (128 equations and outliers removed), and reduced versions with 109 and 89 reactions and the predictions of the minimal model.

The electron density is found to decrease with increasing fraction of CF_4 for all the models. The minimal and full models match each other closely at low CF_4 fraction, but the minimal model predicts a higher electron density at higher fractions. The fewer the number of equations in the reduced model, the higher the prediction of electron density.

Figure 7 compares the prediction of the electron temperature for all the models. For all models, the temperature increases almost linearly with CF_4 fraction. The full model and the reduced model with 109 reactions (Reduced – 1) closely match over most of range of CF_4 fractions. The slope of the electron temperature increase with the CF_4 fraction is lower in the Minimal model than the Full – 1 and Reduced – 1 models.

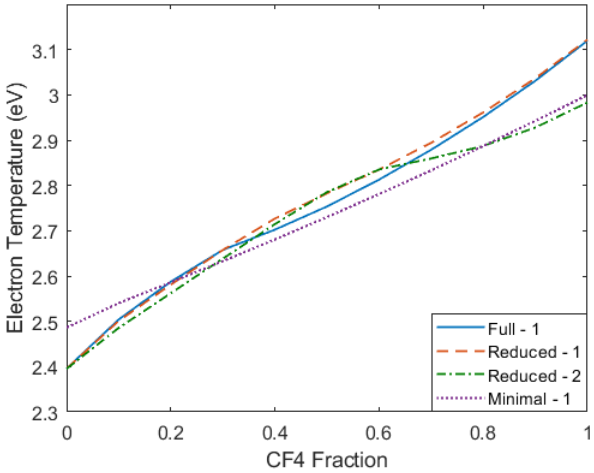

Figure 7. CF4 Fraction versus electron temperature using the Full model (128 equations and outliers removed), and reduced versions with 109 and 89 reactions and the predictions of the minimal model.

4. CONCLUSIONS

A database of experimentally measured kinetic parameters of 128 reactions describing an Ar/CF_4 plasma has been compiled. For several reactions, there are reports of multiple rate constants. In these cases, outliers must be removed before averaging over the remaining rate constants to more closely match experimental measurements of electron density and electron temperature. The full model with outliers removed is then compared to several reduced models, including a minimal 12 reaction model. The predictions of the minimal model miss maxima in the number density of F and CF_3^+, contrary to the full model and reduced models with 109 and 89 reactions. The minimal model is qualitatively and

quantitatively different for predicting these species and requires experimental validation. For the number density of Ar^+, the electron density and the electron temperature, all models are qualitatively similar. In general, the predictions of the full model differ significantly from the reduced models with 109 and 89 reactions and the minimal model. Thus, the incorporation of the full model with all 128 reactions is necessary to describe the Ar/CF_4 plasma.

REFERENCES

[1] W. Guo, and H. H. Sawin, "Review of profile and roughening simulation in microelectronics plasma etching," Journal of Physics D: Applied Physics, 42(19), 194014 (2009).

[2] J. Hoang, C.-C. Hsu, and J. P. Chang, "Feature profile evolution during shallow trench isolation etch in chlorine-based plasmas. I. Feature scale modeling," Journal of Vacuum Science & Technology B: Microelectronics and Nanometer Structures, 26(6), 1911-1918 (2008).

[3] M. J. Kushner, W. Z. Collison, M. J. Grapperhaus *et al.*, "A three-dimensional model for inductively coupled plasma etching reactors: Azimuthal symmetry, coil properties, and comparison to experiments," Journal of Applied Physics, 80(3), 1337 (1996).

[4] C. Lee, and M. A. Lieberman, "Global model of Ar, O2, Cl2, and Ar/O2 high-density plasma discharges," Journal of Vacuum Science & Technology A: Vacuum, Surfaces, and Films, 13(2), 368 - 380 (1995).

[5] A. M. Efremov, G.-H. Kim, J.-G. Kim *et al.*, "Applicability of self-consistent global model for characterization of inductively coupled Cl2 plasma," Vacuum, 81(5), 669-675 (2007).

[6] J. Tennyson, S. Rahimi, C. Hill *et al.*, "QDB: a new database of plasma chemistries and reactions," Plasma Sources Sci. Technol., 26(055014), 2-15 (2017).

[7] M. H. Lee, S. H. Jang, and C. W. Chung, "On the multistep ionizations in an argon inductively coupled plasma," Physics of Plasmas, 13(5), (2006).

[8] K. Ding, M. A. Lieberman, A. J. Lichtenberg *et al.*, "Comparison of a hybrid model with experiments in atmospheric pressure helium and argon capacitive rf discharges," Plasma Sources Science and Technology, 23(6), 065048-065048 (2014).

[9] A. Leblanc, K. Ding, M. A. Lieberman *et al.*, "Hybrid model of atmospheric pressure Ar/O2/TiCl4 radio-frequency capacitive discharge for TiO2 deposition," Journal of Applied Physics, 115(18), (2014).

[10] R. Chanson, A. Rhallabi, M. C. Fernandez *et al.*, "Modeling of inductively coupled plasma Ar/Cl 2 /N 2 plasma discharge: Effect of N 2 on the plasma properties," Journal of Vacuum Science & Technology A: Vacuum, Surfaces, and Films, 31(1), 011301-011301 (2013).

[11] L. Lallement, A. Rhallabi, C. Cardinaud *et al.*, "Global model and diagnostic of a low-pressure SF 6 /Ar inductively coupled plasma," Plasma Sources Science and Technology, 18(2), 25001-25001 (2009).

[12] C. Lazzaroni, and P. Chabert, "A comparison between micro hollow cathode discharges and atmospheric pressure plasma jets in Ar/O ₂ gas mixtures," Plasma Sources Science and Technology, 25(6), 065015-065015 (2016).

[13] J. T. Gudmundsson, and E. G. Thorsteinsson, "Oxygen discharges diluted with argon: dissociation processes," Plasma Sources Science and Technology, 16(2), 399-412 (2007).

[14] E. G. Thorsteinsson, and J. T. Gudmundsson, "A global (volume averaged) model of a Cl2/Ar discharge: I. Continuous power," Journal of Physics D: Applied Physics, 43(11), 115201-115201 (2010).

[15] A. T. Hjartarson, E. G. Thorsteinsson, and J. T. Gudmundsson, "Low pressure hydrogen discharges diluted with argon explored using a global model," Plasma Sources Science and Technology, 19(6), 065008-065008 (2010).

[16] W. Yang, S.-X. Zhao, D.-Q. Wen *et al.*, "F-atom kinetics in SF6/Ar inductively coupled plasmas," Journal of Vacuum Science & Technology A: Vacuum, Surfaces, and Films, 34(3), 031305-031305 (2016).

[17] C.-C. Hsu, M. A. Nierode, J. W. Coburn *et al.*, "Comparison of model and experiment for Ar, Ar/O2 and Ar/O2/Cl2 inductively coupled plasmas," J. Phys D: Appl. Phys., 39(15), 3272-3284 (2006).

[18] T. Kimura, and K. Hanaki, "Experiments and global model analysis of inductively coupled CF 4/O2/Ar plasmas," Japanese Journal of Applied Physics, 47(11), 8537-8545 (2008).

[19] A. Efremov, J. C. Woo, G. H. Kim *et al.*, "Etching characteristics and mechanisms of the MgO thin films in the CF4/Ar inductively coupled plasma," Microelectronic Engineering, 84(4), 638-645 (2007).

[20] A. Efremov, K. H. Kwon, A. Morgunov *et al.*, "Comparative study of CF 4 - and CHF 3 -based plasmas for dry etching applications." 10224, 102241W-102241W.

[21] P. Ho, J. E. Johannes, and R. J. Buss, "Modeling the plasma chemistry of C2F6 and CHF3 etching of silicon dioxide, with comparisons to etch rate and diagnostic data," J. Vac. Sci. Technol. A, 19(5), 2344-2367 (2001).
[22] D. Bose, M. V. V. S. Rao, T. R. Govindan *et al.*, "Uncertainty and sensitivity, analysis of gas-phase chemistry in a CHF3 plasma," Plasma Sources Science & Technology, 12(2), 225-234 (2003).
[23] Y. Kim, S. Kang, Y.-H. Ham *et al.*, "Study on surface modification of silicon using CHF 3 / O 2 plasma for nano-imprint lithography," Journal of Vacuum Science & Technology A: Vacuum, Surfaces, and Films, 30, (2012).
[24] L. G. Christophorou, J. K. Olthoff, and M. V. V. S. Rao, "Electron Interactions with CF 4," Journal of Physical and Chemical Reference Data, 25(5), 1341-1388 (1996).
[25] S. S. Demesh, V. I. Kelemen, and E. Y. Remeta, "Elastic electron scattering by the CF 3 radical in the 1–1000 eV energy range," Journal of Physics B: Atomic, Molecular and Optical Physics, 50, 135201-135201 (2017).
[26] I. Rozum, S. Eden, J. Tennyson *et al.*, "Electron Interaction Cross Sections for CF 3 I , C 2 F 4 , and CF x (1 – 3) Radicals," Journal of Physical and Chemical Reference Data, 35, 267-267 (2006).
[27] I. Rozum, N. J. Mason, and J. Tennyson, "Electron collisions with the CF 3 radical using the R -matrix method," New Journal of Physics, 5, 155.1-155.12 (2003).
[28] J. T. Gudmundsson, "Global model of plasma chemistry in a low-pressure O 2 /F 2 discharge," Journal of Physics D: Applied Physics, 35, 328-341 (2002).
[29] M. V. V. S. Rao, and S. K. Srivastava, "Cross sections for the production of positive ions by electron impact on F2," Journal of Physics B: Atomic, Molecular and Optical Physics, 29, 1841-1848 (1996).
[30] S. Kim, [An Improved Global Model for Electronegative Discharge and Ignition Conditions for Peripheral Plasma Connected to a Capacitive Discharge] University of California at Berkeley, University of California at Berkeley(2006).